의학석사 학위논문

Sublethal copper deficiency during developmental periods induces cerebral aneurysms

발생 시기 구리결핍식이를 통한 뇌동맥류의 발생 유도

2015년 2월

서울대학교 대학원
의학과 뇌신경과학 전공
신 용 원

발생 시기 구리결핍식이를 통한 뇌동맥류의 발생 유도

Sublethal copper deficiency during developmental periods induces cerebral aneurysms

지도교수 이 상 건

이 논문을 의학석사학위논문으로 제출함

2014년 10월

서울대학교 대학원

의학과 뇌신경과학 전공

신 용 원

신용원의 석사학위논문을 인준함

2015년 1월

위 원 장 장 인 진 (인)

부 위 원 장 이 상 건 (인)

위 원 김 만 호 (인)

ABSTRACT

background: Noninvasive pharmacological therapy options are extremely necessary for cerebral aneurysms. To identify the pathophysiological target, we developed an optimal model to review human intracranial aneurysms (IAs).

Methods: Rats were fed copper-free, low-copper, normal, or copper-rich diets at different time periods from gestation to adulthood. The incidences of IAs were evaluated and autopsies were performed to determine the coexistence of cardiovascular diseases.

Results: While rats fed a copper-free diet from gestation were associated with high mortality rates (~80%) resulting from ascending aorta aneurysm rupture, a low-copper diet model led to acceptable mortality rates (~18%) and produced IAs and subarachnoid hemorrhage in about 45% and 9%, respectively. Delayed copper supplementation in the rats primed for copper deficiency from gestation failed to decrease the development of aneurysms. Higher proportion of IAs up to 90% in the rats fed with low-copper diet from gestation period can be easily achieved by flow-augmentation by common carotid artery occlusion and/or hypertension induction with deoxycorticosterone acetate. In addition, we proposed genes involving extracellular matrix and vascular remodeling and some miRNAs as effectors of aneurysm development using this model.

Conclusion: We propose a simple and relevant model of the human IAs by a simple measure to decrease the activity of lysyl oxidases by dietary copper deficiency from gestation. A highly efficacious method to create IAs without any direct manipulation of intracranial arteries would be a powerful tool for future aneurysm studies.

Key words: Animal model; Copper; Intracranial aneurysm; Aortic aneurysm; Gestation

Student Number: 2013-21731

CONTENTS

LIST OF TABLES

LIST OF FIGURES

Introduction

Intracranial aneurysms are found in approximately 3% of the general population and its age distribution is bimodal.[1,2] The older-age peak suggests that old age and vascular risk factors may contribute to developing intracranial aneurysms, whereas the younger-age peak indicates that innate arterial wall fragility may operate.[3-5] A substantial number of patients are naturally aneurysm-prone to have multiple aneurysms[6] and to experience recurrent subarachnoid hemorrhage (SAH) because of aneurysm recurrence and de novo formation, which are more distinctive in pediatric and young adult patients.[7] Therefore, genetic or developmental condition to induce intrinsic wall defects may be a pathogenetic initiator to aneurysm development.

Aneurysmal SAH is a life-threatening condition with high morbidity and mortality; therefore, surgical clipping or endovascular coiling is implemented in asymptomatic cases to prevent rupture.[8] Intriguingly, most intracranial aneurysms remain stable throughout the course of a lifetime, and only a small number of them evolve to being rupture-prone.[9] The current therapeutic options are invasive and have potentially serious complications.[9] In this regard, noninvasive pharmacological therapeutic options are necessary for intracranial aneurysms; however, no therapy has been identified as yet, mainly because of a lack of knowledge about the mechanisms underlying aneurysm development, growth, and rupture. To identify the pathophysiological target, an optimal animal model that manifests cardinal features of human intracranial aneurysms is required. Several models have been proposed using combinations of various pharmacological and surgical methods.[10] While these models show a rapid development of aneurysms and a high rate of rupture, they likely share only small pathways leading to vessel destruction and rupture. There remains a need for more suitable models that exhibit spontaneous development with the least manipulation and that allow stabilization through a healing process, thus harboring multiple unruptured aneurysms with occasional rupture episodes as found in humans.

Although the key element for developing aneurysms is unknown, growing aneurysms are more likely to occur with vessel wall fragility.[11] Elastin and collagen fibers exhibit increased tensile strength that is essential for vessel wall integrity and function, and lysyl oxidases (LOX) are extracellular copper-containing enzymes that stabilize extracellular matrices by cross-linking elastin and collagen monomers into fibers.[12] Copper is an essential micronutrient that is required for the activity of amine oxidases such as LOX.[13] It is recognized that copper deficiency often occurs in infants who consume diets of cow milk and formulas with low copper content and low copper bioavailability.[14-16] Long-term copper deficiency during the developmental period can cause abnormalities of the vascular and skeletal systems; thus, a specific type of copper deficiency from gestation is likely a functional generator of intracranial aneurysm formation.

However, limited information is available regarding the effects of copper deficiency in intracranial aneurysms, and even less is known about the biological mechanisms of copper deficiency in developing intracranial aneurysms. In the present study, we sought to determine whether a certain type of copper deficiency induces intracranial aneurysms relevant to human disease and how this phenotype is achieved.

Materials and Methods

Experimental protocol

To test whether timed copper deficiency during the developmental and growing periods can cause the formation of multiple intracranial aneurysms, we designed a model with rodents fed special diets during certain time periods. The diets included normal diet (ND; AIN-93G Purified Rodent Diet with 6 mg/kg copper; Dyets, Inc., Bethlehem, PA), copper-free diet (CFD; modified AIN-93G Purified Rodent Diet without added copper; Dyets, Inc.), low-copper diet (LCD; Modified AIN-93G Purified Rodent Diet with 2 mg/kg copper; Dyets, Inc.), and copper-rich diet (CRD; Modified AIN-93G Purified Rodent Diet with 30 mg/kg copper; Dyets,

Inc.). Drinking water containing 0.9% saline was administered throughout the experimental period to increase the sympathetic tone. The time periods for the special diets extended from the gestation period to adulthood. The term from mid-pregnancy to birth was referred to as the prenatal period; the 4-week period when pups were kept together with their dam and littermates was referred to as infancy; the 2-month period after separation from the dam was referred to as youth; and the time period after then was referred to as adulthood. For this time schedule, we used pregnant Sprague-Dawley rats (mean gestational age, 12 days; n=14; Dae-Han Bio, Seoul, South Korea) and their pups (n=155). At P21-28, all pups were weaned and randomly housed, with two to three pups in each cage. The experimental model comprised 10 groups according to diet regimen and period. In order to further inhibit the activity of LOX, A LOX inhibitor, 0.12% β -aminopropionitrile (BAPN; Sigma, St. Louis, MO), was added to some laboratory diets.[17] Each group was designated as "A"-"B". The "A" diet was administered during the prenatal period and infancy and the "B" diet was administered during youth and adulthood. Accordingly, the groups were designated and fed as follows: ND-ND (n=7); ND-CFD (n=9); ND-CFD/BAPN (n=15); ND-ND/BAPN (n=13); CFD-ND (n=12); CFD-CFD (n=12); CFD-CFD/BAPN (n=12); CFD-ND/BAPN (n=13); LCD-CFD (n=11); and LCD-CFD/BAPN (n=33). To assess the effect of delayed copper supplementation, two additional groups, LCD-CFD/BAPN-ND (n=15) and LCD-CFD/BAPN-CRD (n=13), were used. These rats were administered ND or CRD for 2 months during adulthood after LCD-CFD/BAPN. The detailed time table for the experimental schedule is provided (Figure 1).

For further development of intracranial aneurysm, we conducted additional experiment by using three induction models: flow-augmented common carotid artery (CCA) occlusion model (left CCA occlusion; n=10), deoxycorticosterone acetate (DOCA)-salt hypertension model (n=7), and left CCA occlusion + DOCA-salt hypertension model (n=10). Rats fed with LCD-CFD/BAPN till adult (ND were administered afterward) were used. For CCA occlusion, rats were anesthetized with isoflurane and left CCA was dissected and ligated immediately

below bifurcation area. For induction of hypertension, DOCA (Sigma, St. Louis, MO) 20mg/kg were subcutaneously injected twice a week and 0.9% saline was supplied as drinking water during experimental period. Autopsy was performed for dead animal and the remained were sacrificed for gross pathological analysis two months after flow-augmentation and/or induction of hypertension. All procedures were performed with institutional approval and were accredited by the Association for the Assessment and Accreditation of Laboratory Animal Care International.

Monitoring

After separation from the mother, rat pups were raised under the same conditions except for diet. The littermates were exposed to the same diet conditions and thus were assigned to the same group. The animals were monitored for survival for 5 months. The diet was prepared nondistinctively and the outcome measure was done independently of the breeder who prepared diet. The cumulative survival statistic was calculated by using Kaplan-Meier statistics. Log-rank *P* value was calculated to compare survival curves. Surviving rats were killed and then subjected to histopathological evaluation and molecular studies at 5 months. To define the natural course of the intracranial aneurysm, some rats fed LCD-CFD/BAPN were killed and then subjected to autopsy and molecular studies at 1, 3, and 5 months after birth.

Histopathology

For dead animals, autopsy was performed immediately at the time of death, and the mortality cause was recorded by gross path ological changes. Because our autopsy data for dead animals showed thoracic hemorrhage or SAH, all rats that survived 5 months were subjected to histopathological studies of the heart, aorta, and brain. Rats were anesthetized and perfused with ice-cold saline, followed by perfusion with a bromophenol blue dye solution (2 mg/mL) dissolved in phosphate-buffered saline and gelatin mixture (20%). The bromophenol blue dye and gelatin mixture was used to delineate pathological changes of the intracranial

arteries. Thoracic cavity, aorta, and arteries of the circle of Willis were examined under a dissecting microscope, and the incidences of aortopathy and intracranial aneurysm were assessed in each group. We defined the aortopathy to describe the development of hemopericardium, hemothorax, ascending thoracic aorta aneurysm, and cardiac hypertrophy. Aneurysm indicated there was obvious outward bulging of the arterial wall compared to its parent artery in macroscopic examination. After examining external features of the major cerebral arteries, the brain tissues were fixed with 4% paraformaldehyde for 24 hours and then cryopreserved as tissue blocks for cryostat sectioning at 30 μm with a cryostat (Leica CM 1900; Leica, Deerfield, IL). Coronal sections were taken at the level of the circle of Willis, which contained the bifurcation of major cerebral arteries. Sections were stained with hematoxylin and eosin to assess the damage to elastic lamina, inflammation, thrombosis, and damage to endothelium, and were stained with Elastica van Gieson to confirm the disappearance of the internal elastic lamina in the macroscopically identified intracranial aneurysms.

Microarray

For the molecular studies, animals were euthanized at 1, 3, and 5 months after birth. As a normal control, age-matched Sprague-Dawley rats fed ND-ND were killed. Samples of the following three categories were then harvested: normal cerebral artery; aneurysm; and parent artery with aneurysm sac. Cerebral artery with aneurysm was carefully dissected free from the surrounding tissues under a dissecting microscope, and then the entire aneurysm was separated from the parent artery. The tissues immediately frozen in liquid nitrogen were stored at −70°C until RNA extraction. After extracting RNA by RNeasy Mini Kit (Qiagen, Valencia, CA), we pooled RNA to generate three test samples per category by combining three RNA samples from each category to decrease the influence of intersample variability. The concentration and quality of each RNA sample were determined using the Agilent 2100 Bioanalyzer (Agilent Technologies, Santa Clara, CA). RNA was labeled and hybridized to Agilent Rat GE v3 microarrays (Agilent

Technologies) as described in the manufacturer's technical manual. Microarrays were scanned with the Agilent DNA microarray scanner (Agilent Technologies), and the scanned images were analyzed using Feature Extraction software (Agilent Technologies) to obtain the signal intensity of the spots. Pooled RNA was also subjected to miRNA microarray. The miRNAs were labeled and hybridized by using the GenoExplorer microRNA array labeling kit and GenoExplorer microRNA chips including 1,088 miRNAs (GenoSensor Corporation, Tempe, AZ). The hybridized microRNA arrays were scanned and analyzed using an Axon GenePix 4000B scanner and GenePix Pro software (Molecular Devices, Sunnyvale, CA). Gene expression was normalized by median normalization methods and presented as the values of the aneurysm and parent artery samples divided by the values of the normal cerebral artery sample. The threshold for differentially regulated genes was set as a two-fold increase or decrease to identify effector genes. The gene functions and associated pathways were evaluated by reviewing Entrez Gene (http://www.ncbi.nlm.nih.gov/sites/entrez?db=gene), Kyoto Encyclopedia of Genes and Genomes (KEGG) database (http://www.genome.jp/kegg/pathway.html), and the published literature.

Results

High early mortality with CFD during the developmental period

In our model, to determine the diet regimen and time point to induce an optimal spontaneous aneurysm, we tested various diet regimens during different time periods (Table 1). Copper deprivation throughout the developmental period and youth produced highly lethal disease, with a 60% mortality rate for rats fed CFD-CFD and 100% mortality rate for rats fed CFD-CFD/BAPN. When we administered the CFD separately during various time points over the course of a lifetime, maternal transfer from CFD during the prenatal period and infancy had the greatest impact on mortality. Most rats fed CFD-CFD or CFD-CFD/BAPN had very rapid disease progression and died within 10 weeks (Figure 2). However, LCD during the perinatal period resulted in low early mortality rates (LCD-CFD, 9%; LCD-CFD/BAPN, 18%) and long-term survival. Although autopsy results demonstrated pericardial and/or thoracic hemorrhage in most rats with little interlitter variability (Figure 3A to D), some additional deaths after 10 weeks were determined to have resulted from SAH (Figure 4B). Thoracic hemorrhage and SAH were thought to occur because of ascending thoracic aorta aneurysm rupture and intracranial aneurysm rupture, respectively.

Long-term vascular outcome with copper-deficient diet

We defined two forms of copper deficiency–related vascular outcomes, aortopathy and intracranial aneurysm. The incidences of aortopathy and intracranial aneurysm according to exposure degree and timing of copper deficiency were evaluated at 5 months after birth (Table 1). Aortopathy developed in virtually all rats fed CFD during their lifetime and highly lethal aortopathy occurred very early, whereas cardiac hypertrophy was detected late in some surviving rats (Figure 3). The incidence of intracranial aneurysms could not be determined because of the high mortality rate. Intracranial aneurysms could be induced frequently in 36% of rats fed LCD-CFD and in 46% of rats fed LCD-CFD/BAPN, resulting in modest

aortopathy rates (8% and 21%, respectively). However, ND during the perinatal period and later copper deficiency showed no pathological changes in the heart, aorta, and thoracic cavity but was associated with intracranial aneurysms in 8% of rats fed ND-BAPN, in 11% of rats fed ND-CFD, and in 33% of rats fed ND-CFD/BAPN.

Morphological features of intracranial aneurysm

LCD during the perinatal period and CFD/BAPN during the youth and adulthood induced intracranial aneurysms in 46.4%. The majority of those aneurysms were stable and unruptured over the course of 5 months and the incidence of SAH was as low as 3.6%. Intracranial aneurysms were distributed uniformly in the arterial bifurcation area of the circle of Willis as single, double, or even triple, and some were associated with internal carotid artery ectasia and basilar artery dolichoectasia, suggesting overall intracranial vascular wall deformity (Figure 5). Histological evaluations showed a breakdown of continuous endothelial cell layer, faint smooth muscle layer, and disorganized elastic lamina (Figure 4). BAPN treatment in combination with CFD changed the disease phenotype from a benign to a severe form, such as rupture or large aneurysm. The mean aneurysm size in LCD-CFD/BAPN rats (915.4±137.3 μm) was significantly larger than that in LCD-CFD rats (713.7±108.2 μm; $P<0.001$).

Increased efficacy of IA development through flow-augmentation and/or hypertension induction

For further development of intracranial aneurysm, flow-augmentation by CCA occlusion, hypertension induction by DOCA-salt model, or both were used. Two of the rats in the DOCA-salt model group died, one with SAH and the other with unclear cause but without rupture in the intracranial or aortic arteries. Eight (80%) of 10 in the CCA occlusion group showed intracranial aneurysms including 1 ruptured aneurysm at the junction of basilar artery and vertebral artery (Figure 6A). Five (71.4%) of 7 in the DOCA-salt model group showed intracranial

aneurysms including 1 SAH. CCA occlusion + DOCA-salt model resulted in highest proportion (90%) of rats with intracranial aneurysm. Compared to the other rat models, these three groups showed apparently higher proportion of intracranial aneurysms with more prominent vascular change in some rats (Figure 6B), which indicates that normal looking arteries also have intrinsic arteriopathy susceptible to aneurysmal change under stress condition.

Molecular signature of intracranial aneurysm

To obtain a global view of the changes in gene expression in the intracranial aneurysm, we performed gene expression arrays in the intracranial aneurysm and its parent artery samples (n=3 per group). Each sample was pooled from ND-ND, LCD-CFD, and LCD-CFD/BAPN groups of rats at age 5 months. Of approximately 35,000 genes, we analyzed differentially upregulated and downregulated genes of the aneurysm and parent artery compared with the normal artery. There were small proportions of differentially regulated genes in the aneurysm compared to the normal artery (3,659 genes). Remarkably, both aneurysm and parent artery expressed similar patterns of differentially upregulated genes compared with normal artery (Figure 7A). When the ontology of those genes was determined, significant genes involved extracellular matrix, immune and inflammatory responses, neural crest cell differentiation, and blood vessel remodeling (Tables 2-4). In the category of significantly downregulated genes, the largest changes were for genes involved in extracellular matrix signaling, including collagen type 1, collagen type 3, collagen type 6, elastin, fibrillin 1, fibrillin 2, LOX, LOXL1, and LOXL2 (Figure 7B and 8). To further understand the epigenetic change potentially affecting the gene expression or stability, we identified miRNA differentially expressed in the aneurysm. Compared with normal artery, intracranial aneurysm had significantly reduced expression of six miRNAs and increased expression of 18 miRNAs (Table 5). Although the aneurysm and parent artery showed similar miRNA expression patterns, some miRNAs were differentially upregulated.

Effect of late supplementation of CRD on aneurysm development

Next, we investigated whether the delayed copper supplementation could attenuate the development of intracranial aneurysm. Copper was supplemented with ND (6 mg/kg copper) or CRD (30 mg/kg copper) for 2 months after 3 months of LCD-CFD/BAPN. Although mortality was not found, aortopathy was noted in 13.3% and 15.3% of rats fed LCD-CFD/BAPN-ND and LCD-CRD, respectively, and intracranial aneurysms were found in 46.6% and 46.1%, respectively. As compared with the continued CFD/BAPN group, the delayed copper supplementation failed to alter the disease progression. To predict the time of disease onset, we also tracked serial changes of molecular signatures during the youth and adulthood. Despite the gradual increase in development of intracranial aneurysms over time, most significantly regulated genes and miRNAs had already been altered from 1 month of age, although there was a more positive or negative trend as time passed (Figures 7C and D).

Discussion

The most significant finding of this study is that copper deficiency during the developmental period induces a variety of vascular wall abnormalities involving thoracic aorta aneurysms and intracranial aneurysms. The disease phenotype and severity were dependent on the degree and timing of copper deficiency. Although the concept of copper deficiency was applied simply to attenuate the LOX activity, target vessels went through a wide range of genetic and epigenetic changes that could not be altered by late copper supplementation. This is the first preclinical study to show the common pathogenetic basis of intracranial aneurysm and aorta pathology, to provide a highly relevant model of human cerebral aneurysm, and to provide a great deal of information to enable future research to access its therapeutic target.

LOX has a critical role in the matrix assembly.[12] LOX requires one tightly bound copper at its active site,[13] and its activity in growing animals is influenced directly by the amount of dietary copper.[17] Because adequate copper status and functional LOX are essential in early stages of vascular development,[18,19] we created our model by feeding the dams a copper-deficient diet starting from pregnancy and by feeding the offspring the same diet for 4 weeks after birth. In some rats, BAPN was added to further accentuate the decreased LOX activity by copper deficiency.[20] Phenotypes of our model varied according to the intensity and duration of the deficiency. Severely copper-deficient rats died of hemopericardium and hemothorax during youth or died of cardiac failure during adulthood. Ascending thoracic aortas were dilated with distortion and depletion of elastic fibers, and the hearts were hypertrophied. However, mortality may have been the result of the differential impact on development of multiple organs, because copper also operates in other essential enzyme systems as a cofactor.[21] The clinical relevance of our model relates to the fact that cow milk and some homemade infant formulas have insufficient copper levels and are unfavorable for bioavailability and utilization of copper.[14-16] Moreover, several lines of evidence suggest the average daily intake of copper in Western diets is lower than what is recommended to be adequate.[22,23] More individuals than expected may experience long-term suboptimal copper status starting from the early developmental period and, perhaps, are at risk for development of aortopathy and intracranial aneurysms.

Intracranial aneurysms are frequently subjected to therapeutic challenges because of the low risk of rupture and invasiveness of current therapies;[24] therefore, the most practical steps in intracranial aneurysm research are to define a high-risk aneurysm and to identify a therapeutic target for noninvasive treatment. However, our knowledge of the mechanisms leading to aneurysm development, progression, and rupture is greatly limited because we always find only a final phenotype in humans. Therefore, investigators have made an effort to develop an animal model to examine the entire course of intracranial aneurysms. Oral

chemical agents to induce wall fragility slowly were initially tried in rats and primates, but the incidence of intracranial aneurysms was low, the size was disproportionally small, and the histological changes were subtle and without any arterial wall bulging.[20, 25-27] These observations are in line with our data indicating that BAPN-only treatment during adulthood produced intracranial aneurysms in only 7.7%. The next attempt used multiple chemical or mechanical methods to injure healthy arteries, and these trials were associated with a high rate of mortality and rupture rate within a very short time period.[28,29] However, the applied methods and outcomes were quite different from what occurs in the human condition, and it was difficult to assess effects of pharmacological treatment on the phenotype because the efficacy was dependent on whether the drug was specific to each injury component rather than overall pathophysiology. Given that intracranial aneurysms result mainly from a mismatch in the matrix assembly of the tunica media and hemodynamic stress,[9,30] we attempted to weaken the integrity of the vascular wall by long-term sublethal copper-deficient diet and drinking water containing 0.9% saline starting from the pregnancy and lactation periods. Intracranial aneurysms were multiple, macroscopically distinguishable, and detected in 45% of the experimental group and the proportion could be increased up to 90% by flow-augmentation and/or hypertension induction. Histopathological features included a discontinuation of elastic lamina, loss of cellular components, and disorganization of muscle fiber structure. Although most aneurysms were stabilized as unruptured aneurysms, in some aneurysms the vascular wall was further weakened, eventually resulting in aneurysmal rupture. Because of the simplicity of the model, large aneurysms, high incidence of aneurysms, and acceptable mortality, the sublethal copper-deficient model would be suitable for high-throughput studies to determine critical pathways participating in the pathophysiology of intracranial aneurysms.

Although most intracranial aneurysms remain stable through some healing process, some aneurysms display odd features, including multiplicity, large size, and rupture presentation as small aneurysm.[3,31] It is speculated that the latter is

partly related to the developmental abnormality of artery wall. Some hints about the concept of innate wall deformity are obtainable from our model, which is characterized by the concurrent development of aortopathy and intracranial aneurysm. The cervicocephalic muscular arteries are derived from the neural crest, which also participates in cardiac development and outflow valves.[32] Thus, an abnormality of the neural crest may be the common pathogenetic factor in ascending thoracic aorta aneurysm and intracranial aneurysm.[33,34] The relatively weak association between abdominal aortic aneurysm and intracranial aneurysm[35] further supports the theory of neurocristinopathy, because the abdominal aorta is clearly different from the thoracic aorta and cervicocephalic artery in origin, structure, and function of the vascular wall.[36] The ultimate duties of neural crest–derived mesenchymal cells are to compose and stabilize the tunica media of arteries via matrix production and assembly.[36] Thus, it appears reasonable that the alteration in matrix assembly induces the pathology in the ascending thoracic aorta and intracranial artery walls, as found in our model.

Although the exact underlying mechanisms are not fully known, several factors including extracellular matrix integrity, inflammation, and endothelial maintenance have been suggested to be involved in the formation and/or rupture of intracranial aneurysm.[37] Although copper deficiency was primarily intended to alter the LOX activity in our study, various changes in cell motility and migration, cell signaling, and transcriptional regulation were also anticipated because LOX affects intracellular dynamics in an extracellular matrix–independent manner.[11, 12] As expected, our microarray analysis of aneurysms identified expression changes for various genes involved in endothelial matrix formation and blood vessel remodeling, several of which (i.e., COL1A2, COL3A1, COL5A2, elastin, fibrillin 1, and fibrillin 2 have been implicated as effectors of aneurysm development.[37,38] Moreover, our study also identified altered expression of miRNAs. Although the functions of significant miRNAs are yet to be fully elucidated, distinctly expressed miRNAs could be linked to the alteration of the extracelluar matrix and vessel remodeling. Our unique animal model could be a

promising tool to further dissect the epigenetic machinery surrounding aneurysm development, growth, and rupture.

Cerebral aneurysms are thought to be acquired lesions that develop and grow over the course of a lifetime, and they rupture when the matrix of the aneurysm wall becomes too fragile to resist the hemodynamic pressure.[30] Serial analyses of gene and miRNA expression revealed that the significant gene changes have already occurred from the early growing period and become more prominent in adulthood. Therefore, it may be a matter of course that late copper supplementation is not effective for reducing the development of aneurysms. Future therapeutic strategies should be applied to regulate the epigenetic changes underlying aneurysm development.

References

1. Vlak MH, Algra A, Brandenburg R, Rinkel GJ. Prevalence of unruptured intracranial aneurysms, with emphasis on sex, age, comorbidity, country, and time period: a systematic review and meta-analysis. Lancet Neurol 2011;10:626-636.

2. Risselada R, de Vries LM, Dippel DW, van Kooten F, van der Lugt A, Niessen WJ, et al. Incidence, treatment, and case-fatality of non-traumatic subarachnoid haemorrhage in the Netherlands. Clin Neurol Neurosurg 2011;113:483-487.

3. Schievink WI, Mokri B, Piepgras DG, Gittenberger-de Groot AC. Intracranial aneurysms and cervicocephalic arterial dissections associated with congenital heart disease. Neurosurgery 1996;39:685-689.

4. Alg VS, Sofat R, Houlden H, Werring DJ. Genetic risk factors for intracranial aneurysms: a meta-analysis in more than 116,000 individuals. Neurology 2013;80:2154-2165.

5. Yasuno K, Bakırcıoğlu M, Low SK, Bilgüvar K, Gaál E, Ruigrok YM, et al. Common variant near the endothelin receptor type A (EDNRA) gene is associated with intracranial aneurysm risk. Proc Natl Acad Sci U S A 2011;108:19707-19712.

6. Rinne J, Hernesniemi J, Puranen M, Saari T. Multiple intracranial aneurysms in a defined population: prospective angiographic and clinical study. Neurosurgery 1994;35:803–808.

7. Koroknay-Pál P, Niemelä M, Lehto H, Kivisaari R, Numminen J, Laakso A, et al. De novo and recurrent aneurysms in pediatric patients with cerebral aneurysms. Stroke 2013;44:1436-1439.

8. Nieuwkamp DJ, Setz LE, Algra A, Linn FH, de Rooij NK, Rinkel GJ. Changes in case fatality of aneurysmal subarachnoid haemorrhage over time, according to age, sex, and region: a meta-analysis. Lancet Neurol 2009;8:635-642.

9. Wiebers DO, Whisnant JP, Huston J 3rd, Meissner I, Brown RD Jr, Piepgras DG, et al. Unruptured intracranial aneurysms: natural history, clinical outcome, and risks of surgical and endovascular treatment. Lancet 2003;362:103-110.

10. Bouzeghrane F, Naggara O, Kallmes DF, Berenstein A, Raymond J; International Consortium of Neuroendovascular Centres. In vivo experimental intracranial aneurysm models: a systematic review. AJNR Am J Neuroradiol 2010;31:418-423.
11. Chalouhi N, Ali MS, Jabbour PM, Tjoumakaris SI, Gonzalez LF, Rosenwasser RH, et al. Biology of intracranial aneurysms: role of inflammation. J Cereb Blood Flow Metab 2012;32:1659-1676.
12. Liu X1, Zhao Y, Gao J, Pawlyk B, Starcher B, Spencer JA, et al. Elastic fiber homeostasis requires lysyl oxidaselike 1 protein. Nat Genet 2004;36:178-182.
13. Gacheru SN, Trackman PC, Shah MA, O'Gara CY, Spacciapoli P, Greenaway FT, et al. Structural and catalytic properties of copper in lysyl oxidase. J Biol Chem 1990;265:19022-19027.
14. Lönnerdal B, Bell JG, Keen CL. Copper absorption from human milk, cow's milk, and infant formulas using a suckling rat model. Am J Clin Nutr 1985;42:836-844.
15. Lönnerdal B. Copper nutrition during infancy and childhood. Am J Clin Nutr 1998;67:1046S-1053S.
16. Suskind DL. Nutritional deficiencies during normal growth. Pediatr Clin North Am 2009;56:1035-1053.
17. Opsahl W, Zeronian H, Ellison M, Lewis D, Rucker RB, Riggins RS. Role of copper in collagen cross-linking and its influence on selected mechanical properties of chick bone and tendon. J Nutr 1982;112:708-716.
18. Jankowski MA, Uriu-Hare JY, Rucker RB, Keen CL. Effect of maternal diabetes and dietary copper intake on rat fetus development. Reprod Toxicol 1993;7:589-598.
19. Harris ED. A requirement for copper in angiogenesis. Nutr Rev 2004;62:60-64.
20. Hashimoto N, Kim C, Kikuchi H, Kojima M, Kang Y, Hazama F. Experimental induction of cerebral aneurysms in monkeys. J Neurosurg 1987;67:903-905.

21. Zatta P, Frank A. Copper deficiency and neurological disorders in man and animals. Brain Res Rev 2007;54:19-33.
22. Pennington JA, Schoen SA. Total diet study: estimated dietary intakes of nutritional elements, 1982-1991. Int J Vitam Nutr Res 1996;66:350-362.
23. Brewer GJ. Copper in medicine. Curr Opin Chem Biol 2003;7:207-212.
24. Sato K, Yoshimoto Y. Risk profile of intracranial aneurysms: rupture rate is not constant after formation. Stroke 2011;42:3376-3381
25. Handa H, Hashimoto N, Nagata I, Hazama F. Saccular cerebral aneurysms in rats: a newly developed animal model of the disease. Stroke 1983;14:857-866.
26. Hashimoto N, Handa H, Hazama F. Experimentally induced cerebral aneurysms in rats. Surg
Neurol 1978;10:3-8.
27. Hashimoto N, Handa H, Hazama F. Experimentally induced cerebral aneurysms in rats: part II.
Surg Neurol 1979;11:243-246.
28. Morimoto M, Miyamoto S, Mizoguchi A. Mouse model of cerebral aneurysm: experimental induction by renal hypertension and local hemodynamic changes. Stroke 2002;33:1911-1915.
29. Nuki Y, Tsou TL, Kurihara C, Kanematsu M, Kanematsu Y, Hashimoto T. Elastase-induced intracranial aneurysms in hypertensive mice. Hypertension 2009;54:1337-1344.
30. Frösen J, Tulamo R, Paetau A, Laaksamo E, Korja M, Laakso A, et al. Saccular intracranial aneurysm: pathology and mechanisms. Acta Neuropathol 2012;123:773-786.
31. Matsubara S1, Hadeishi H, Suzuki A, Yasui N, Nishimura H. Incidence and risk factors for the growth of unruptured cerebral aneurysms: observation using serial computerized tomography angiography. J Neurosurg 2004;101:908-914.
32. LeDouarin NM, Kalcheim C. The neural crest. 2nd ed. Cambridge: Cambridge University Press, 1999.
33. Tadros TM, Klein MD, Shapira OM. Ascending aortic dilatation associated

with bicuspid aortic valve: pathophysiology, molecular biology, and clinical implications. Circulation 2009;119:880-890.
34. Schievink WI, Raissi SS, Maya MM, Velebir A. Screening for intracranial aneurysms in patients with bicuspid aortic valve. Neurology 2010;74:1430-1433.
35. Kuzmik GA, Feldman M, Tranquilli M, Rizzo JA, Johnson M, Elefteriades JA. Concurrent intracranial and thoracic aortic aneurysms. Am J Cardiol 2010;105:417-420.
36. Lindsay ME, Dietz HC. Lessons on the pathogenesis of aneurysm from heritable conditions. Nature 2011;473:308-316.
37. Li L, Yang X, Jiang F, Dusting GJ, Wu Z. Transcriptome-wide characterization of gene expression associated with unruptured intracranial aneurysms. Eur Neurol 2009;62:330-337.
38. Kilic T, Sohrabifar M, Kurtkaya O, Yildirim O, Elmaci I, Günel M, et al. Expression of structural proteins and angiogenic factors in normal arterial and unruptured and ruptured aneurysm walls. Neurosurgery 2005;57:997-1007.

Table 1. Model summary

Model	N	Diet				Mortality, %	Aortopathy,%*	ICA, %†
		Prenatal	Infant	Youth (≤3 Months)	Adult (4-5 Months)			
ND-ND	7	ND	ND	ND	ND	0	0	0
ND-CFD	9	ND	ND	CFD	CFD	0	0	11.1
ND-CFD/BAPN	15	ND	ND	CFD/BAPN	CFD/BAPN	6.7	0	33.3
ND-ND/BAPN	13	ND	ND	BAPN	BAPN	0	0	7.7
CFD-ND	12	CFD	CFD	ND	ND	0	0	0
CFD-CFD	12	CFD	CFD	CFD	CFD	58.3	58.3	N/D
CFD-CFD/BAPN	12	CFD	CFD	CFD/BAPN	CFD/BAPN	100	100	N/D
CFD-ND/BAPN	13	CFD	CFD	ND/BAPN	ND/BAPN	7.7	16.7	8.3
LCD-CFD	11	LCD	LCD	CFD	CFD	9.1	0	36.3
LCD-CFD/BAPN	33	LCD	LCD	CFD/BAPN	CFD/BAPN	18.1	21.2	46.4
LCD-CFD/BAPN-ND	15	LCD	LCD	CFD/BAPN	ND	0	13.3	46.6
LCD-CFD/BAPN-CRD	13	LCD	LCD	CFD/BAPN	CRD	0	15.3	46.1

BAPN, β-aminopropionitrile; CFD, copper-free diet (0 mg/kg copper); CRD, copper-rich diet (30 mg/kg copper); ICA, intracranial aneurysm; LCD, low-copper diet (2 mg/kg copper); N/D, not determined; ND, normal diet (6 mg/kg copper).

Aortopathy includes pericardial tamponade, thoracic hemorrhage, ascending thoracic aorta aneurysm, or cardiac hypertrophy.

*Incidence of aortopathy in total number of rats.

†Incidence of intracranial aneurysms in rats that survived.

Table 2. Genes related to extracellular matrix

Gene name*	Expression ratio		
	Aneurysm/Normal	Parent/Normal	Aneurysm/Parent
cathepsin G	0.069	0.067	1.032
elastin	0.116	0.126	0.917
insulin-like growth factor 1	0.118	0.135	0.872
dermatopontin	0.158	0.287	0.550
SPARC related modular calcium binding 2	0.158	0.175	0.904
dermatopontin	0.158	0.287	0.550
collagen, type I, alpha 1	0.163	0.185	0.879
ADAM metallopeptidase with thrombospondin type 1 motif, 12	0.181	0.185	0.976
carboxypeptidase X (M14 family), member 2	0.181	0.224	0.808
fibrillin 2	0.185	0.170	1.084
SPARC related modular calcium binding 2	0.188	0.180	1.044
lysyl oxidase	0.198	0.243	0.816
ADAMTS-like 3	0.227	0.241	0.943
hemicentin 1	0.234	0.277	0.846
fibrillin 1	0.254	0.287	0.884
Fibrillin 1	0.254	0.287	0.884
lysyl oxidase-like 1	0.255	0.293	0.871
nidogen 2	0.260	0.329	0.792
lectin, galactoside-binding, soluble, 3	0.264	0.450	0.586
collagen, type III, alpha 1	0.272	0.347	0.784
collagen, type VI, alpha 1	0.274	0.331	0.826
microfibrillar associated protein 5	0.290	0.399	0.728
ADAMTS-like 3	0.291	0.325	0.894
collagen, type V, alpha 2	0.291	0.338	0.859
transforming growth factor, beta induced	0.291	0.341	0.854
collagen, type VI, alpha 2	0.301	0.351	0.858
lysyl oxidase-like 2	0.302	0.369	0.818
EGF-containing fibulin-like extracellular matrix protein 1	0.311	0.364	0.854
collagen, type IV, alpha 5	0.312	0.366	0.851
ADAM metallopeptidase with thrombospondin type 1 motif, 7	0.312	0.337	0.926
Kazal-type serine peptidase inhibitor domain 1	0.314	0.341	0.921
nidogen 2	0.314	0.292	1.075
collagen, type V, alpha 2	0.320	0.373	0.858
ADAM metallopeptidase with thrombospondin type 1 motif, 5	0.325	0.383	0.848
periostin, osteoblast specific factor	0.342	0.317	1.077
collagen, type XIV, alpha 1	0.342	0.435	0.787
peroxidasin homolog (Drosophila)	0.351	0.384	0.915
decorin	0.357	0.464	0.770
thrombospondin, type I, domain containing 4	0.377	0.408	0.924
matrix metallopeptidase 19	0.385	0.516	0.745
somatomedin B and thrombospondin, type 1 domain containing	0.398	0.475	0.839
bone morphogenetic protein 4	0.399	0.507	0.788
complement factor properdin	0.399	0.529	0.755
collagen, type XII, alpha 1	0.401	0.450	0.890

collagen, type I, alpha 2	0.415	0.455	0.912
ADAM metallopeptidase with thrombospondin type 1 motif, 14	0.417	0.187	2.226
collagen, type XII, alpha 1	0.425	0.487	0.872
vitrin	0.427	0.396	1.078
transforming growth factor, beta receptor II	0.428	0.484	0.883
ADAM metallopeptidase with thrombospondin type 1 motif, 10	0.428	0.506	0.847
filamin A, alpha	0.430	0.442	0.974
smooth muscle alpha-actin	0.442	0.593	0.746
matrix metallopeptidase 16	0.444	0.499	0.890
bone morphogenetic protein 7	0.445	0.501	0.888
fibromodulin	0.445	0.524	0.849
wingless-type MMTV integration site family, member 11	0.449	0.522	0.860
wingless-type MMTV integration site family, member 10A	0.449	0.447	1.004
wingless-type MMTV integration site family, member 5A	0.451	0.458	0.984
myosin, heavy chain 11, smooth muscle	0.474	0.551	0.861
collagen, type XII, alpha 1	0.474	0.566	0.837
elastin microfibril interfacer 1	0.482	0.540	0.892
versican	0.548	0.710	0.772
reelin	2.140	2.550	0.839
Norrie disease (pseudoglioma) (human)	3.635	4.020	0.903
wingless-type MMTV integration site family, member 3	3.734	3.196	1.168
glutamate receptor, ionotropic, N-methyl D-aspartate 1	3.820	3.090	1.236
EF hand domain family, member B	4.054	3.925	1.033
matrix metallopeptidase 24	4.107	3.730	1.102
fibroblast growth factor 9	4.621	4.651	0.993
zona pellucida glycoprotein 2 (sperm receptor)	5.998	5.503	1.090
EGF-like-domain, multiple 6	7.210	7.060	1.020
acetylcholinesterase	7.710	8.880	0.867
RELT-like 2	10.614	11.900	0.895
tenascin R	11.973	14.800	0.809
protein tyrosine phosphatase, receptor-type, Z polypeptide 1	12.831	14.200	0.906
sparc/osteonectin, cwcv and kazal-like domains proteoglycan (testican) 1	13.780	26.500	0.520
brevican	23.500	25.200	0.932

*The altered genes in the level of the expression are classified and grouped between the aneurysm (n=3) and the normal cerebral artery (n=3). The criteria are a more than 2-fold changes in the ratio of aneurysm to normal and a statistical difference (P<0.01, Student's t-test) between aneurysm and control. Parent artery indicates normally appearing artery in the aneurysm model.

Table 3. Genes related to immune response and inflammatory response

Gene name*	Expression ratio		
	Aneurysm/Normal	Parent/Normal	Aneurysm/Parent
cathepsin G	0.069	0.067	1.032
free fatty acid receptor 4	0.083	0.109	0.757
chemokine (C-C motif) ligand 12	0.106	0.195	0.546
centromere protein F	0.115	0.114	1.012
ficolin B	0.126	0.161	0.784
chemokine (C-C motif) ligand 4	0.159	0.203	0.781
cyclin-dependent kinase 1	0.168	0.222	0.756
epoxide hydrolase 2, cytoplasmic	0.168	0.325	0.518
killer cell lectin-like receptor subfamily K, member 1	0.198	0.345	0.574
chemokine (C-X-C motif) ligand 13	0.216	0.237	0.912
tumor necrosis factor	0.232	0.331	0.700
chemokine (C-X-C motif) ligand 10	0.245	0.445	0.551
dipeptidylpeptidase 4	0.288	0.323	0.891
Fc fragment of IgG, low affinity IIIa, receptor	0.298	0.425	0.702
chemokine (C-C motif) ligand 6	0.308	0.451	0.683
UDP-Gal:betaGlcNAc beta 1,4-galactosyltransferase, polypeptide 1	0.310	0.333	0.932
ectonucleotide pyrophosphatase/phosphodiesterase 1	0.310	0.379	0.818
acid phosphatase 5, tartrate resistant	0.312	0.324	0.963
chemokine (C-C motif) ligand 6	0.319	0.463	0.689
PML-RARA regulated adaptor molecule 1	0.324	0.338	0.960
adenosine deaminase	0.327	0.418	0.782
complement component 5a receptor 1	0.327	0.431	0.759
inhibitor of kappa light polypeptide gene enhancer in B-cells, kinase epsilon	0.331	0.327	1.012
solute carrier family 7 (cationic amino acid transporter, y+ system), member 2	0.331	0.373	0.888
phosphodiesterase 5A, cGMP-specific	0.339	0.412	0.823
chemokine (C motif) ligand 1	0.344	0.445	0.774
cytochrome b-245, beta polypeptide	0.365	0.349	1.046
endothelin receptor type A	0.370	0.387	0.957
RT1 class I, locus CE10	0.380	0.376	1.011
chemokine (C-C motif) ligand 7	0.382	0.467	0.819
caspase 6	0.387	0.501	0.772
B and T lymphocyte associated	0.389	0.449	0.867
PYD and CARD domain containing	0.393	0.512	0.767
somatomedin B and thrombospondin, type 1 domain containing	0.398	0.475	0.839
complement factor properdin	0.399	0.529	0.755
endothelin receptor type A	0.401	0.445	0.901
spleen tyrosine kinase	0.405	0.369	1.097
protein tyrosine phosphatase, receptor type, C	0.412	0.473	0.871
mannan-binding lectin serine peptidase 1	0.413	0.380	1.087
hemochromatosis	0.417	0.378	1.103
G protein-coupled receptor 183	0.420	0.462	0.908
C-type lectin domain family 4, member A	0.426	0.541	0.789
myosin IF	0.428	0.538	0.796

complement factor H	0.429	0.496	0.864
adrenoceptor beta 2, surface	0.430	0.465	0.924
toll-like receptor 4	0.431	0.565	0.763
interleukin 15	0.434	0.501	0.867
C-type lectin domain family 7, member A	0.435	0.551	0.790
interleukin-1 receptor-associated kinase 3	0.446	0.539	0.826
interleukin 1 receptor antagonist	0.447	0.455	0.983
myeloid differentiation primary response 88	0.447	0.581	0.769
interferon regulatory factor 3	0.449	0.464	0.966
Fc fragment of IgG, high affinity Ia, receptor (CD64)	0.450	0.593	0.758
wingless-type MMTV integration site family, member 5A	0.451	0.458	0.984
5' nucleotidase, ecto	0.451	0.530	0.850
CD1d1 molecule	0.452	0.532	0.850
G-protein signaling modulator 3	0.457	0.586	0.779
interleukin 18	0.459	0.564	0.814
2 ' -5 ' oligoadenylate synthetase 1F	0.459	0.648	0.709
unc-93 homolog B1 (C. elegans)	0.461	0.601	0.766
protein tyrosine phosphatase, non-receptor type 6	0.461	0.570	0.809
platelet factor 4	0.463	0.540	0.856
transporter 2, ATP-binding cassette, sub-family B (MDR/TAP)	0.467	0.642	0.728
SP110 nuclear body protein	0.468	0.559	0.838
toll-like receptor 2	0.468	0.628	0.745
MHC class I polypeptide-related sequence B	0.470	0.419	1.122
signal transducer and activator of transcription 6	0.471	0.514	0.916
NCK associated protein 1 like	0.471	0.636	0.741
G protein-coupled receptor 183	0.473	0.533	0.887
tumor necrosis factor receptor superfamily, member 1a	0.473	0.512	0.924
hemopexin	0.474	0.594	0.798
tumor necrosis factor (ligand) superfamily, member 10	0.475	0.539	0.882
Fc fragment of IgE, high affinity I, receptor for; gamma polypeptide	0.480	0.651	0.737
Fc fragment of IgG, high affinity Ia, receptor (CD64)	0.481	0.575	0.838
histamine receptor H4	0.481	0.462	1.040
ADAM metallopeptidase domain 17	0.484	0.515	0.941
opioid receptor, mu 1	0.493	0.703	0.701
Cd55 molecule	0.496	0.605	0.820
complement component 3a receptor 1	0.496	0.523	0.949
Thy-1 cell surface antigen	2.021	1.738	1.162
adenosine A1 receptor	2.399	2.441	0.982
arginase type II	2.490	2.458	1.015
bone morphogenetic protein receptor, type IB	2.685	2.780	0.967
coagulation factor II (thrombin) receptor	2.762	3.468	0.796
cell adhesion molecule 1	3.460	3.600	0.961
semaphorin 7A, GPI membrane anchor	3.540	3.970	0.891
forkhead box J1	4.330	6.771	0.640
mitogen activated protein kinase 10	4.460	4.310	1.035

cytochrome P450, family 11, subfamily b, polypeptide 1	5.270	4.181	1.260
CD24 molecule	5.914	6.810	0.868
chemokine (C-X-C motif) ligand 14	8.519	8.610	0.990
carbohydrate (keratan sulfate Gal-6) sulfotransferase 1	8.799	9.090	0.968
chitinase, acidic	10.552	7.877	1.340
fatty acid binding protein 4, adipocyte	11.230	11.000	1.017
aquaporin 4	21.500	25.200	0.851

*The altered genes in the level of the expression are classified and grouped between the aneurysm (n=3) and the normal cerebral artery (n=3). The criteria are a more than 2-fold changes in the ratio of aneurysm to normal and a statistical difference (P<0.01, Student's t-test) between aneurysm and normal cerebral artery. Parent artery indicates normally appearing artery in the aneurysm model.

Table 4. Genes related to neural crest cell differentiation and blood vessel remodeling

Gene name	Expression ratio		
	Aneurysm/Normal	Parent/Normal	Aneurysm/Parent
dipeptidylpeptidase 4	0.276	0.311	0.888
hypothetical protein LOC681382	0.293	0.284	1.032
TBC1 domain family, member 22a	0.294	0.934	0.315
baculoviral IAP repeat-containing 5	0.307	0.406	0.756
guanylate binding protein 5	0.322	0.403	0.798
Zic family member 2	0.327	0.496	0.659
Zic family member 1	0.369	0.419	0.880
Zic family member 4	0.385	0.433	0.890
branched chain amino acid transaminase 2, mitochondrial	0.387	0.426	0.909
Zic family member 5	0.427	0.460	0.927
T-box18	0.430	0.490	0.878
similar to CG7194-PA	0.445	0.526	0.846
G-protein signaling modulator 3	0.457	0.586	0.779
potassium inwardly-rectifying channel, subfamily J, member 12	0.465	0.459	1.013
glycolipid transfer protein domain containing 2	0.479	0.774	0.619
activin A receptor, type I	0.493	0.489	1.047
forkhead box D3	0.499	0.920	0.553
telomerase RNA component	2.105	2.011	1.047
serine peptidase inhibitor, Kunitz type 1	3.123	2.998	1.042
crystallin, gamma B	3.181	0.900	3.534
sparc/osteonectin, cwcv and kazal-like domains proteoglycan (testican) 2	3.260	3.080	1.056
frizzled family receptor 9	3.490	2.933	1.191
cystathionine beta synthase	6.240	9.140	0.682
membrane-associated ring finger (C3HC4) 11	6.840	6.904	0.991
pterin-4 alpha-carbinolamine dehydratase/dimerization cofactor of hepatocyte nuclear factor 1 alpha	11.106	13.500	0.823
fatty acid binding protein 4, adipocyte	11.230	11.000	1.017
dendrin	17.300	11.170	1.549
iroquois homeobox 1	17.405	20.500	0.850

*The altered genes in the level of the expression are classified and grouped between the aneurysm (n=3) and the normal cerebral artery (n=3). The criteria are a more than 2-fold changes in the ratio of aneurysm normal cerebral artery normal and a statistical difference (P<0.01, Student's t-test) between aneurysm and control. Parent artery indicates normally appearing artery in the aneurysm model.

Table 5. Profiles of significant miRNA in intracranial aneurysm

miRNA*	Expression ratio		
	Aneurysm/Normal	Parent/Normal	Aneurysm/Parent
miR-675-3p	0.087	0.072	1.206
miR-10a-3p	0.217	0.634	0.343
miR-199a-5p	0.394	0.363	1.087
miR-142-3p	0.432	0.427	1.011
miR-542-3p	0.450	0.407	1.103
miR-542-5p	0.489	0.418	1.169
miR-505-5p	2.402	1.992	1.206
miR-300-5p	2.564	2.424	1.058
miR-34c-5p	2.665	1.663	1.603
miR-9a-3p	3.083	2.476	1.265
miR-873-5p	3.726	2.630	1.417
miR-380-5p	4.086	2.919	1.400
miR-342-5p	4.599	4.871	0.944
miR-376c-3p	4.690	3.337	1.405
miR-92b-3p	5.081	1.461	3.587
miR-139-5p	6.156	3.995	1.541
miR-129-5p	6.195	4.982	1.244
miR-187-3p	6.606	3.135	2.107
miR-7b	7.710	5.606	1.375
miR-193-5p	9.726	2.049	4.747
miR-485-5p	23.289	13.203	1.764
miR-1298	28.968	4.086	7.090
miR-106b-3p	59.128	1.351	43.760
miR-499-3p	94.172	8.010	11.757

*The altered miRNAs in the level of the expression are grouped between the aneurysm (n=3) and the normal cerebral artery (n=3). The criteria are a more than 2-fold changes in the ratio of aneurysm to normal and a statistical difference (P<0.01, Student's t-test) between aneurysm and normal cerebral artery. Parent artery indicates normally appearing artery in the aneurysm model.

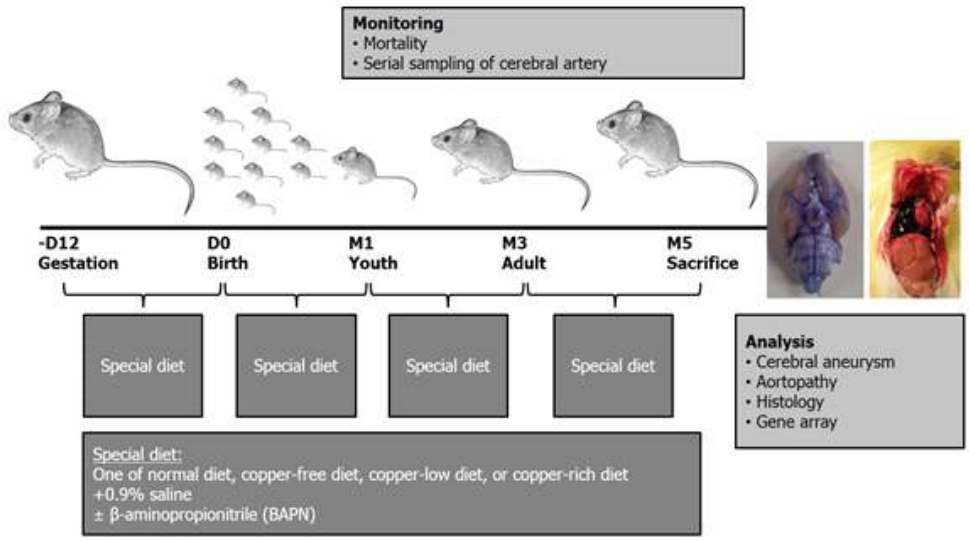

Figure 1. Time table showing the experimental schedule. Our experiment spanned from gestation to early adulthood in rats. Rats were administered different diets, including normal diet (6 mg/kg copper), copper-free diet (0 mg/kg copper), low-copper diet (2 mg/kg copper), and copper-rich diet (30 mg/kg copper) during different time periods. Mortality rate and incidence of cerebral aneurysm and aortopathy were monitored over the course of 5 months. Intracranial aneurysm and parent cerebral arteries were subjected to gene and morphological analyses.

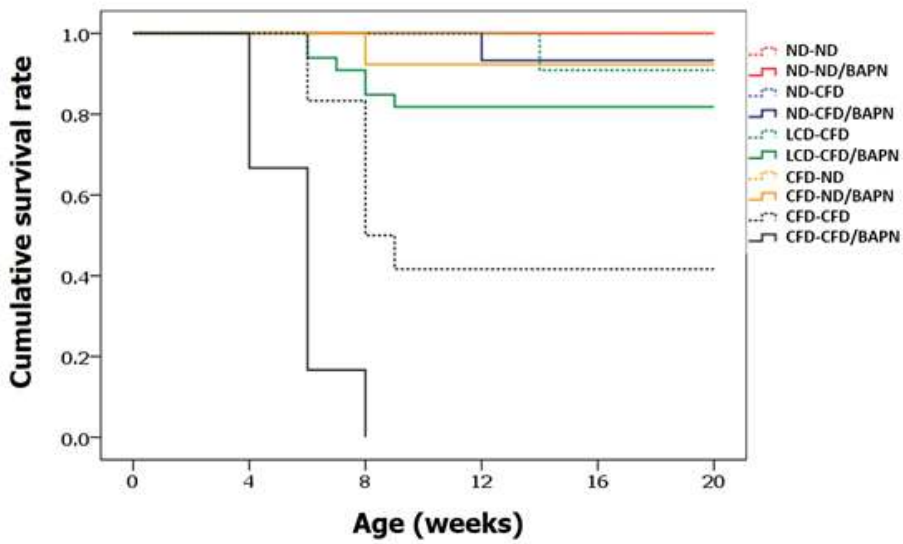

Figure 2. Kaplan-Meier survival curve for various experimental models. Kaplan-Meier analysis estimated the rate of death over the course of 20 weeks among rats with special diets during the perinatal period,youth and adulthood. "A" diet was administered during the perinatal period and "B" diet was administered during the youth and adulthood. The differences between groups were significant (P<0.001, log-rank test). BAPN, β-aminopropionitrile; CFD, copper-free diet; CRD, copper-rich diet (30 mg/kg copper); LCD, low-copper diet (2 mg/kg copper); ND, normal diet.

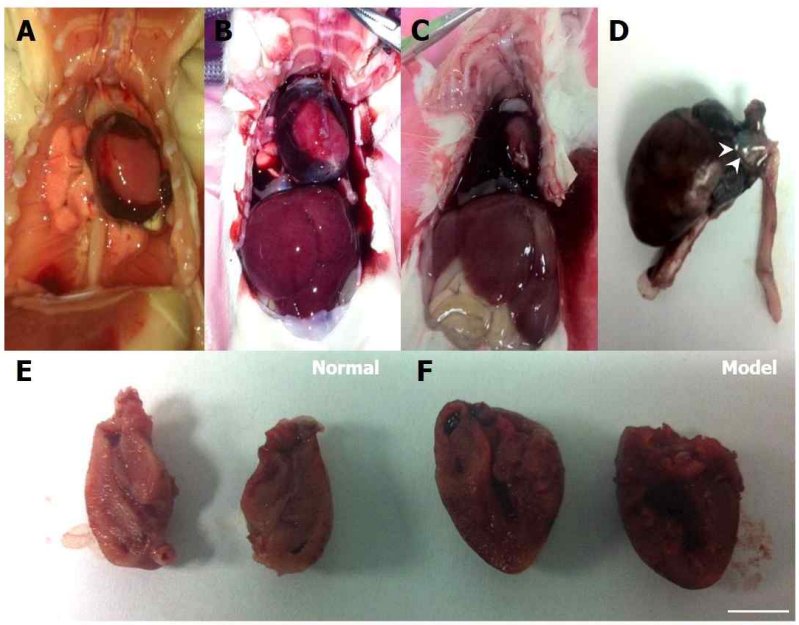

Figure 3. Aortopathy development. Photos of rats fed copper-free diet starting from the gestation period showing various phenotypes of aortopathy. For each rat, including dead and living rats, the chest wall was opened and examined for pericardial effusion (A), pericardial hematoma (B), hemothorax (C), ascending thoracic aorta aneurysm (D, arrowheads), and cardiomegaly (E, F). The main causes of early mortality were thought to be pericardial tamponade, mediastinum compression, and hemodynamic shock by ascending thoracic aorta rupture. The heart was sliced coronally at the level of the interventricular septum to examine the myocardium hypertrophy. Comparing with normal heart (E), cardiomegaly and myocardium hypertrophy were frequently combined with aortopathy in the copper-free diet model (F). Bar represents 5 mm.

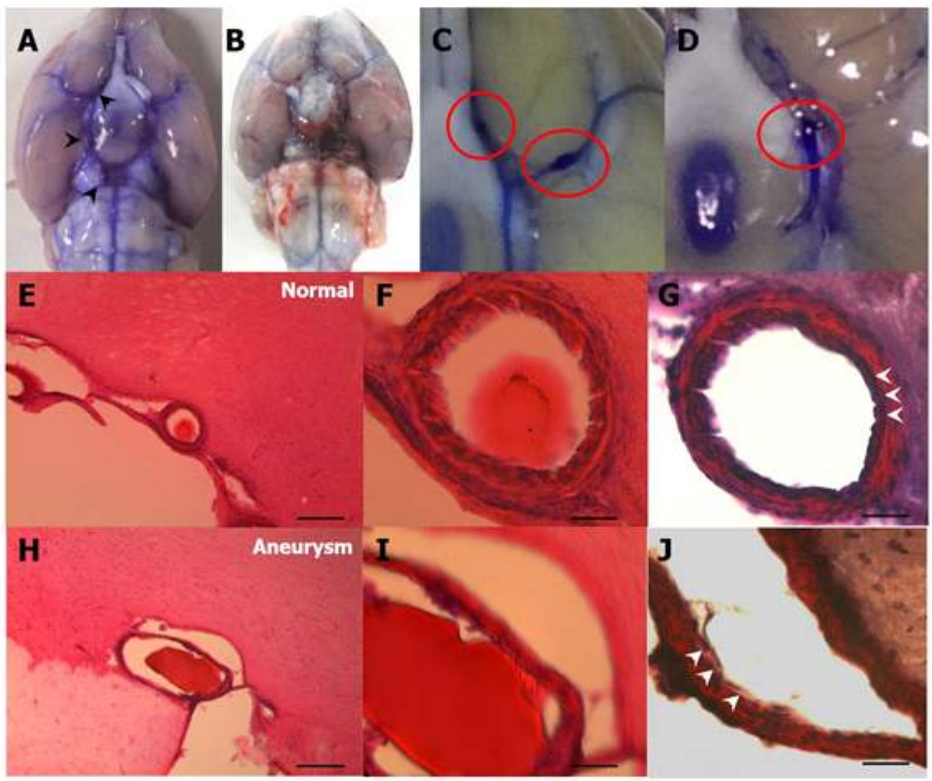

Figure 4. Intracranial aneurysm development. Rats were killed by cardiac perfusion with bromophenol blue dye plus gelatin to delineate the artery structure. Low-copper diet or copper-free diet during the developmental period induced multiple intracranial aneurysms (A, black arrowheads). A few rats experienced subarachnoid hemorrhage, leading to a sudden death (B). Intracranial aneurysms occurred mainly in the arterial bifurcation area (C, D). Hematoxylin and eosin staining showed a single, continuous layer of endothelial cells and two to three layers of smooth muscle cells in the normal cerebral artery. Elastica van Gieson (G) staining showed one layer of elastic lamina (white arrowheads). In an intracranial aneurysm (H and I), discontinued endothelial cell layer and faint smooth muscle layer were noted. Elastica van Gieson staining revealed profoundly disorganized elastic lamina (J). Bars represent 300 μm (E, H) and 50 μm (F, G, I, J).

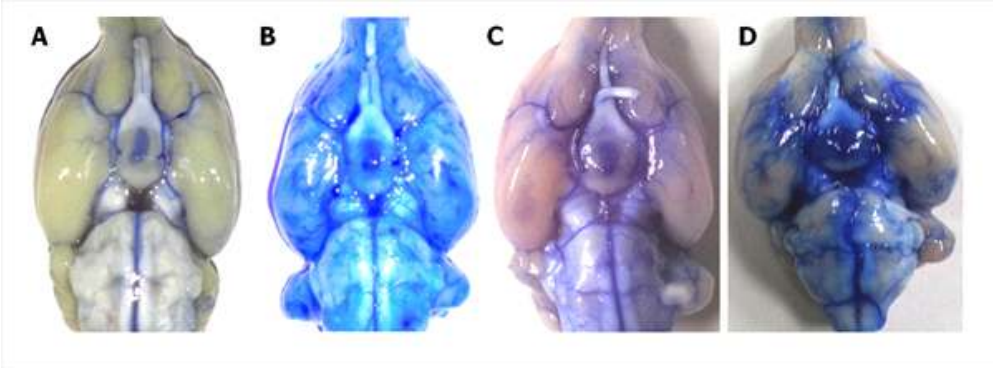

Figure 5. Various phenotypes of abnormal cerebral arteries in the intracranial aneurysm model. Copper-low or -free diet during the developmental period induced various phenotypes of abnormal cerebral arteries. We found rats with solitary aneurysm (A), multiple aneurysms (B), internal carotid artery ectasia (C), and basilar artery dolichoectasia (D).

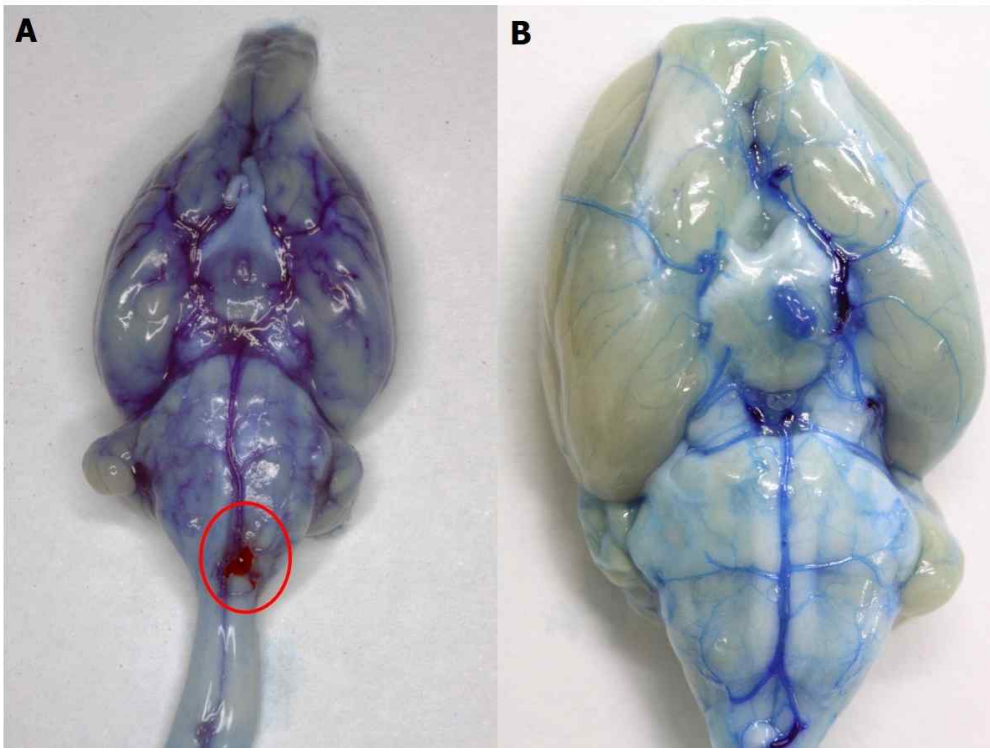

Figure 6. Intracranial aneurysm induction by flow-augmentation and/or DOCA-salt hypertension model. Rats fed with LCD-CFD/BAPN underwent CCA occlusion and/or injected with DOCA twice a day with supplementation of 0.9% salt containing drinking water. One of the rat underwent CCA occlusion showed ruptured intracranial aneurysm at the junction between basilar artery and vertebral artery (A). Prominent vascular changes with several intracranial aneurysms after both CCA occlusion and DOCA-salt hypertension induction for 2 months are exemplified in (B).

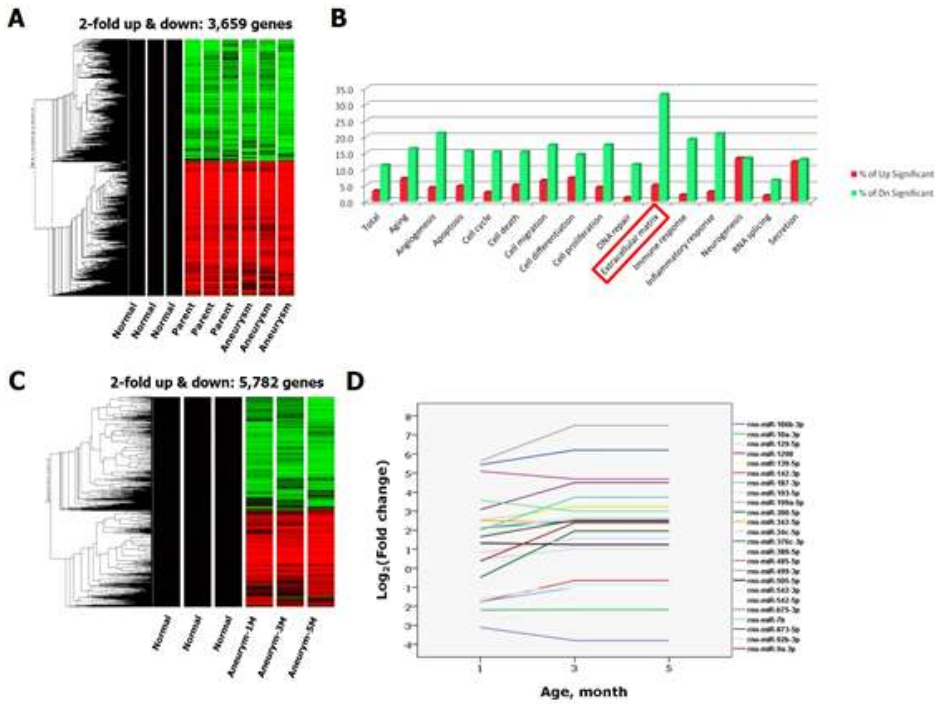

Figure 7. Gene and miRNA expression in intracranial aneurysm. Gene expression was analyzed by microarray in the intracranial aneurysm and parent artery of 5-month-old rats after copper-deficient diet compared with cerebral artery of age-matched normal rats. Heat map shows 3,659 upregulated and downregulated genes as defined by a more than two-fold change in expression (P<0.05) in comparison to those of the normal rats (A). Colors indicate the z-score, with red indicating higher expression (higher z-score) and green indicating lower expression. Significantly upregulated and downregulated genes in the intracranial aneurysm were classified according to gene ontology, and gene-related extracellular matrix was robustly decreased in the aneurysm (B). When gene expression was serially analyzed in the intracranial aneurysm, there were 5,782 upregulated and downregulated genes, as defined by a more than two-fold change in expression (P<0.05) compared to normal rats (C). miRNA expression was also analyzed by microarray in the same sample. Graph (D) depicts miRNAs that were significantly upregulated and downregulated during the aneurysm induction period. Time points

for arrays are plotted on the x-axis, and the expression intensities of miRNAs in the aneurysm in comparison to those of the normal rats are plotted on the y-axis (n=3 per group).

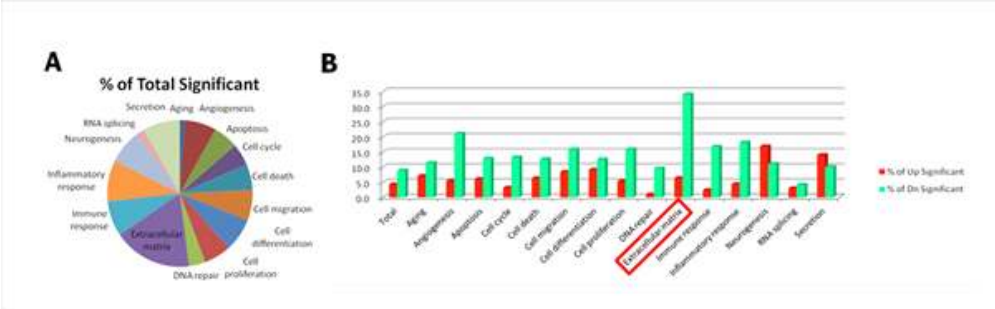

Figure 8. Ontology of significant genes in the parent artery of intracranial aneurysm model vs. normal artery. Significantly upregulated and downregulated genes in the parent artery of intracranial aneurysm model were classified according to gene ontology (B), and genes related extracellular matrix were robustly decreased in the nonaneurysmal parent artery compared to normal artery (C). n=3 per group.

국문초록

배경: 뇌동맥류에 대한 비침습적 약물치료 방법의 개발은 매우 중요하다. 이를 위해서 본 연구에서는 뇌동맥류의 병리 메커니즘을 밝혀 치료의 타깃을 찾기 위한 새로운 뇌동맥류 모델을 개발하였다.

방법: 임신기부터 발생 시기 동안 쥐들에게 구리완전결핍식이, 구리부족식이, 정상식이 및 구리풍부식이를 서로 다른 시기에 공급한 뒤 부검을 통하여 뇌동맥류의 발생을 관찰하였으며 이와 함께 심혈관계 질환 여부도 같이 관찰하였다.

결과: 임신기간부터 구리완전결핍식이를 공급받았던 쥐들의 경우 주로 상행대동맥류 파열로 인한 높은 사망률(~80%)을 보였으나, 구리부족식이를 사용한 쥐들의 경우 사망률은 ~18% 수준이었다. 이 쥐들에서 뇌동맥류 및 지주막하출혈을 각각 45% 및 9% 정도에서 관찰할 수 있었으며 이후 구리 공급을 정상화 하더라도 뇌동맥류의 발생 비율을 줄일 수는 없었다. 또한, 총경동맥 결찰 또는 deoxycorticosterone acetate를 통해 고혈압을 유도한 경우 최대 90%의 쥐에서 뇌동맥류를 발생시킬 수 있었다. 이에 더하여 본 모델을 이용하여 뇌동맥류 발생과 연관되어있는 세포외기질, 혈관재형성 등과 관련된 유전자 및 miRNA들을 제시하였다.

결론: 본 연구에서는 임신기부터 구리 섭취량을 줄임으로써 lysyl oxidase의 작용을 저해하여 뇌동맥류를 유도하는 간단한 모델을 제시하였다. 이는 뇌혈관을 직접 건드리지 않으면서 높은 효율로 뇌동맥류를 유도할 수 있는 방법으로 추후 뇌동맥류 연구에 활용가치가 높을 것이다.

주요어: 동물 모델, 구리, 뇌동맥류, 대동맥류, 임신기

학번: 2013-21731